Available online at www.sciencedirect.com

SciVerse ScienceDirect

Ceramics International 39 (2013) 3857–3864

CERAMICS INTERNATIONAL

www.elsevier.com/locate/ceramint

Adsorption and adhesion of poly(vinyl alcohol) and poly(ammonium acrylate) as organic additives for wet mold processing of Al_2O_3

Toshihiro Isobe[a,*], Mari Nakanome[a], Kazuko Nakazono[b], Sachiko Matsushita[a], Akira Nakajima[a]

[a]Department of Metallurgy and Ceramics Science, Tokyo Institute of Technology, Tokyo, Japan
[b]Department of Organic and Polymeric Materials, Tokyo Institute of Technology, Tokyo, Japan

Received 30 August 2012; received in revised form 18 October 2012; accepted 18 October 2012
Available online 26 October 2012

Abstract

Adsorption and adhesion of polyvinyl alcohol (PVA) molecules on Al_2O_3 surfaces in pH 3–10 or 0–0.1 mass% poly(ammonium acrylate) (PAA) aqueous solution was examined using the AFM colloidal probe method. The PVA behavior on the solid surface was estimated using force curve measurements obtained using colloidal probe AFM. Extensions originating from the bridging of PVA between the solid surfaces were observed primarily at less than approximately 200 nm in the pH 3 aqueous solution. The extensions, which were observed at more than approximately 600 nm for pH 6 and 10 aqueous solutions, resulted from different conformations of the PVA molecules. In the PVA–PAA system, the number of extensions decreased by increasing the PAA content. This was not observed in a PAA aqueous solution of greater than 0.1 mass%, which indicates that PAA was adsorbed selectively onto the solid surface. The force curve showed that PAA was more effective than PVA.

Keywords: A. Suspensions; D. Al_2O_3

1. Introduction

Wet molding processing is traditionally used to fabricate ceramic products [1]. Recently, it has also been applied to the solid freeform fabrication [2,3] and self-assembly processes [4], particularly in optics and for energy devices, including solar cells [5–9]. Dispersion and agglomeration properties of the colloids are widely known to be closely related to the properties of the final products. This relation has been studied carefully for a long time. Fundamentally, colloidal behavior in an aqueous solvent is explained using the Derjaguin–Landau–Verwey–Overbeek (DLVO) theory [10]. However, some interaction forces are not predicted by this classical theory (non-DLVO force). Colloids coated with organic polymers typically exhibit a non-DLVO force because the electrical double-layer thickness in a solvent is usually much less than that of the polymer adsorption layer [11]. Furthermore, because of polymer adsorption, the Hamaker constant and the radius of the colloids, which are important factors for the DLVO theory, cannot be estimated. Consequently, polymer additives confer complex rheological properties to slurries.

Polymer additives have generally been categorized as binders, plasticizers, and dispersants [12]. The effects associated with additives of these different types have been demonstrated primarily using rheological tests. The results have greatly enhanced the understanding of slurries and pastes as a continuum and have contributed importantly to chemical engineering and powder technology. However, little discussion has been conducted of the effects in relation to surface science. Evaluations of the polymer behavior on colloids in a solvent are expected to improve colloid processes considerably because polymer behavior can exert control over dispersion and agglomeration.

During the past several decades, rapid progress has taken place in colloidal probe techniques used for atomic

*Correspondence to: 2-12-1 Ookayama, Meguro-ku, Tokyo, 152-8550, Japan. Tel.: +81 3 5734 3355; fax: +81 3 5734 2525.
E-mail address: isobe.t.ad@m.titech.ac.jp (T. Isobe).

0272-8842/$ - see front matter © 2012 Elsevier Ltd and Techna Group S.r.l. All rights reserved.
http://dx.doi.org/10.1016/j.ceramint.2012.10.228

force microscopy (AFM) in solvents [13–17]. This technique also analyzes the behavior of polymer additives in solvents [18–27]. Scherer et al. reported that carboxymethylcellulose exhibits a bridging force in a poor solvent [18]. Bridging and steric forces between ZrO_2 surfaces in polyacrylic acid were observed by Biggs [19]. The interaction forces are reportedly dependent on the surface coverage of the polymer at the solid–aqueous interface. Yilmaz et al. also measured the bridging force of methylcellulose [20]. These polymers have been used widely as binders. It is expected that the bridging forces obtained from AFM results are related to the rheological properties of suspensions including such polymers as binders. Kauppi et al. studied ethylene oxide working as a dispersant on MgO surfaces [21]. Polyethyleneimine (PEI) has been studied carefully by Kakui et al., who described the relation between the rheological properties of the ceramics–water–PEI system and the force curve results [22]. We have also reported observations of repulsive forces between the solid surfaces in poly(ammonium acrylate) (PAA) [23,24]. Other interactions were also estimated using the AFM force curve mode [26,27].

The research described above primarily addressed one kind of polymer. However, in some studies, polymer additives were mixed and added to a slurry in a general colloid process or were added to pH-controlled solutions. The results from these studies indicate that the polymer additives exhibit more complex behavior on the colloid surface. These evaluations can potentially improve the colloid process. In this study, we first focused on the adsorption and adhesion of polyvinyl alcohol (PVA) molecules on Al_2O_3 surfaces to ascertain the role of PVA in the suspension. Then, we evaluated the PAA–PVA system. This system, used previously for ceramic processes [28], is regarded as a model of the colloid process. The behaviors of PVA, a typical binder, and PAA, a commercial dispersant, on the Al_2O_3 surface were estimated as a function of pH.

2. Materials and methods

2.1. Materials

For this study, PVA (Avg. Mn: 2000; Wako Pure Chemical Industries Ltd., Osaka, Japan), PAA (Celuna D-305; Chukyo Yushi Co. Ltd., Aichi, Japan), a sapphire wafer with a (0001) orientation (SA100510; Aki Corporation, Japan), and commercial Al_2O_3 beads (CB-A10; Showa Denko K.K., Tokyo, Japan) were used. The PVA was 98 mol% hydrolyzed, and 2 mol% acetate groups remained. HCl and NaOH (Wako Pure Chemical Industries Ltd., Osaka, Japan) solutions were employed to adjust the pH of the solution and slurries. Ion-exchanged purified water was distilled using a water purifier (Auto still, Model WG-250; Yamato Scientific Co. Ltd., Tokyo, Japan).

The Al_2O_3 colloidal probes were prepared from Al_2O_3 beads with a particle size of approximately 10 μm (CB-A10; Showa Denko K.K., Tokyo, Japan), tipless triangle cantilevers (PNP-TR-TL-50; Nanoworld AG, Switzerland), and epoxy glue (Araldite ♯1600; Showa Highpolymer Co. Ltd., Tokyo, Japan) using a micromanipulator (Model M331; Suruga Seiki Co. Ltd., Shizuoka, Japan). The spring constant was 0.08 N/m.

2.2. Preparation and properties of the Al_2O_3 suspension

First, 0.001–0.1 mass% PVA and/or PAA were mixed with ion-exchanged purified water. Then, 2 mass% Al_2O_3 beads were dispersed in the solutions. A suspension consisting of only 2 mass% Al_2O_3 beads and ion-exchanged purified water was also prepared. Finally, the pH was adjusted to 3.0, 6.0, and 10.0 by adding a solution of either HCl or NaOH.

Zeta potentials were measured using commercial apparatus (ELS-Z; Otsuka Electronics Co. Ltd., Osaka, Japan). The zeta potential of the Al_2O_3 beads was measured. The suspensions were diluted at an Al_2O_3/liquid ratio of 0.1 g/L and dispersed by ultrasonication for 15 min. Then, the pH was adjusted by adding a solution of either HCl or NaOH. The zeta potential measurement was also conducted after PVA adsorption. The Al_2O_3 beads and the sapphire wafers were soaked in a 0.1 mass% PVA aqueous solution for 24 h. The zeta potential of the soaked samples was measured.

The amount of PVA and PAA adsorbed onto the Al_2O_3 beads was calculated from the difference between the PVA and PAA concentrations before and after the adsorption experiment. The samples were obtained using centrifugation of the suspension at 8000 rpm for 10 min. The initial and absorbed PVA and PAA concentrations were measured using a total organic carbon analyzer (TOC; TOC-V CSH; Shimadzu Corp., Kyoto, Japan). The suspensions were steeped in liquid nitrogen for approximately 5 min. The frozen samples were then dried using a freeze dryer (DC 400; Yamato Scientific Co. Ltd., Tokyo, Japan) at −45 °C for 2 days. The microstructures of the obtained lumps were observed using a field-emission scanning electron microscope (FE-SEM; S4500; Hitachi High-Technologies Corp., Tokyo, Japan).

2.3. Force curve measurements

A sapphire wafer was cut into approximately 1×3 cm^2 plates before cleaning with acetone and ethanol for 15 min. After drying, the substrates were immersed in an O_3 atmosphere at room temperature for 15 min to remove organics. Force curve measurements were performed using a scanning probe microscope (SPM; JSPM-5200; JEOL Ltd., Tokyo, Japan). The Al_2O_3 colloidal probes and one sapphire wafer plate were set up as described in a previous report for measurements in a liquid. The obtained raw data were converted into force–distance (separation between the probe and surface) curves [23,24].

The zeta potential of the sapphire wafer was also estimated using the previously described apparatus with

an attachment to measure the substrate. To estimate the adsorption of PAA on the sapphire surface, a static contact angle measurement was also conducted (Dropmaster 500; Kyowa Interface Science Co. Ltd., Saitama, Japan). First, the cleaned wafer was soaked in approximately 60 mL of the 0–1 mass% PAA aqueous solution for 1 h to avoid the adsorption/desorption of PAA during contact angle measurement. The concentrations of the PAA aqueous solution for both the soaking and the contact angle measurement were the same.

3. Results and discussion

3.1. Effect of pH on PVA adsorption on Al_2O_3

Before AFM colloidal probe measurement, the PVA adsorption behavior was observed using zeta potential measurement, the solution depletion method, and FE-SEM. Fig. 1 shows the relation between pH and the zeta potential. The respective isoelectric points (IEPs) of the Al_2O_3 beads and sapphire wafer were approximately 8.9 and 6.2. The zeta potentials of the Al_2O_3 beads at pH 4.0 and 10.0 were approximately 41.8 and −32.1 mV, respectively. The zeta potentials of the samples at pH 6.0 were also positive. In contrast, after the adsorption of PVA, the surface charge approached zero. Fig. 2 shows the adsorbed amount of PVA on the Al_2O_3 beads estimated using the TOC analyzer. The adsorption amount increased proportionally with the PVA concentration. These results indicate that PVA was adsorbed onto the Al_2O_3 beads and sapphire wafers. Generally, the adsorption isotherm of PVA was fitted by the Langmuir equation, assuming monolayer PVA adsorption on the surfaces of the Al_2O_3 powder. In contrast,

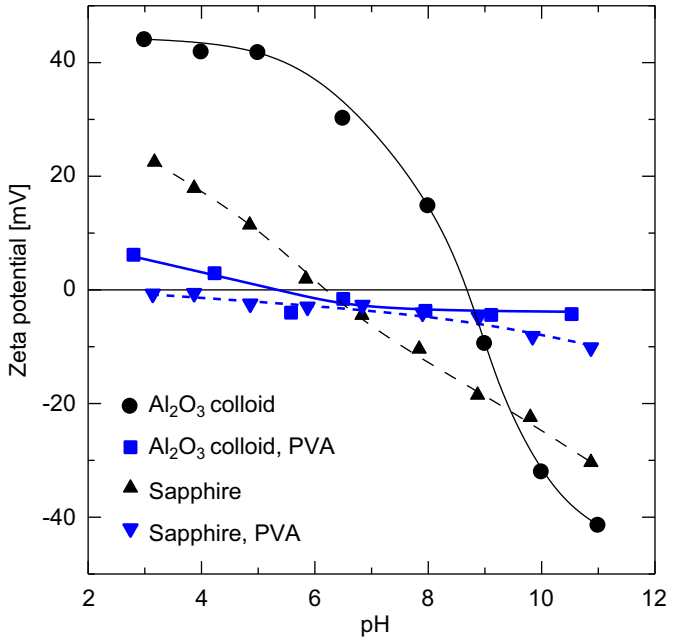

Fig. 1. Zeta potential of the Al_2O_3 beads and the raw sapphire substrate before and after adsorption of PVA as a function of pH.

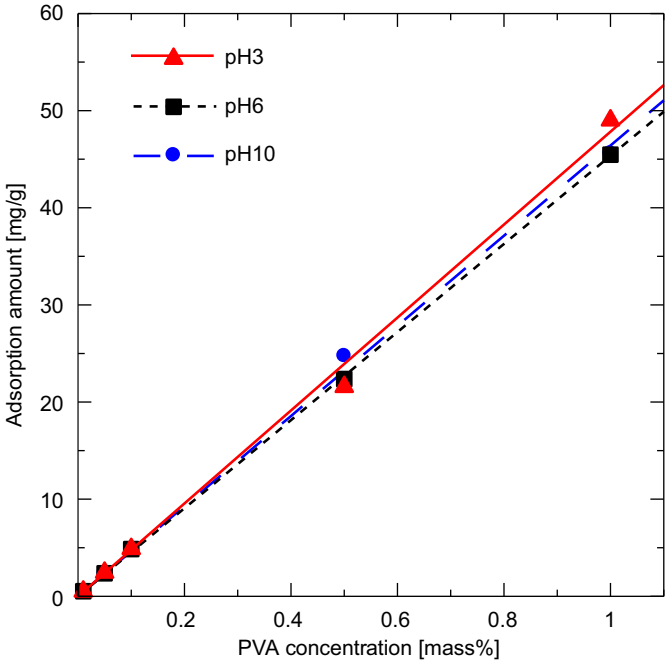

Fig. 2. PVA adsorption amount as a function of PVA concentration.

micrometer-sized Al_2O_3 was used in this study; the adsorption site is very small, and PVA is adsorbed as a multilayer. This state was also observed by FE-SEM. Fig. 3 portrays FE-SEM images of the freeze-dried samples. The PVA, which has a thin thread shape, was entangled between particles at pH 3 and 6. The PVA at pH 3 was slightly thinner than that at pH 6. Moreover, at pH 10, the swollen sheet-shaped PVA was adsorbed onto the Al_2O_3 surface. However, at pH 3, while most PVA chains were adsorbed flatly onto the Al_2O_3 surface, the minority formed thin threads. At pH 10, the electrostatic repulsion between the PVA chains and the solid surface moves the stretched conformation toward the liquid phase. Consequently, PVA were shaped as a sheet. The conformation of PVA at pH 6 was a structure between that of PVA at pH 3 and 10. However, the conformation is apparently more similar to that at pH 3.

3.2. Evaluation of the PVA adhesion

Fig. 4 shows the relation between separation distance and normalized force measured using the AFM colloidal probe method in the 0.1 mass% PVA aqueous solutions. At distances greater than 200 nm, a smooth line was observed at approximately 0 mN m^{-1} in the pH 3 solution. However, extensions were obtained at approximately 150 and 200 nm. It is considered that these extensions originate from the bridging of PVA between the sapphire surface and the Al_2O_3 colloidal probe because polymers that adhere to both solid surfaces are lost after some stretching [20]. The shape of the force curve changes relative to pH. The distance between the extensions was greater at pH 6 and 10. To elucidate these differences, the separation

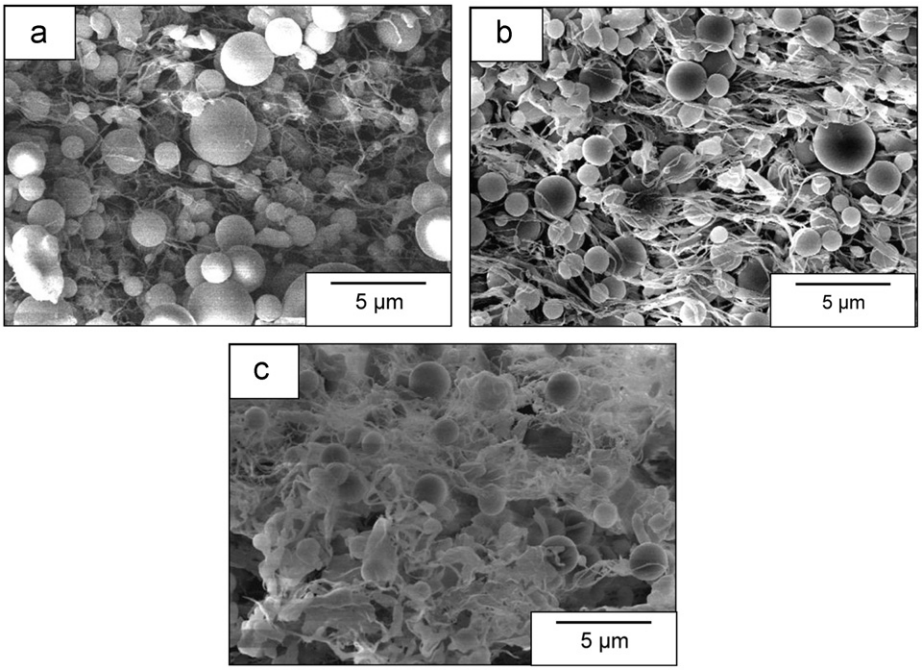

Fig. 3. FE-SEM micrograph of the suspension after freeze–drying. The pH of the suspension was (a) 3, (b) 6, and (c) 10.

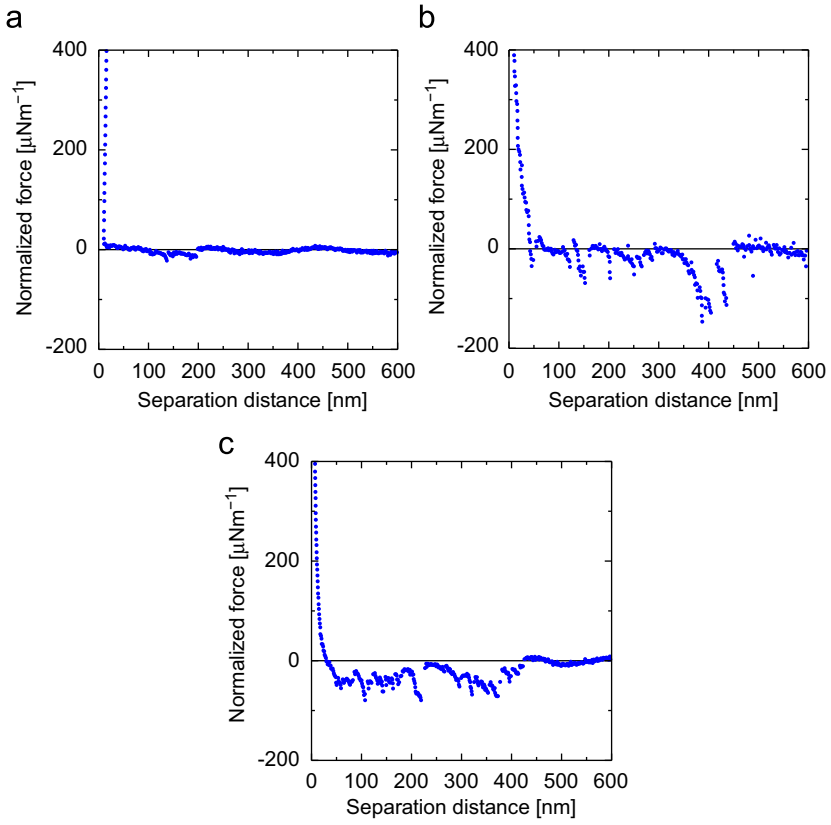

Fig. 4. Force curves measured in the 0.1 mass% PVA aqueous solution droplet. The pH of the suspension was (a) 3, (b) 6, and (c) 10.

distance distributions of the extensions were estimated. First, force curves were measured 50 times in each pH solution. The separation distances at the end of the extensions were read. Then, the separation distance distributions of the extensions were estimated, as presented in Fig. 5. The respective numbers of the extension events were 127, 1095, and 691 for pH 3, 6, and 10, which indicates that, among the three different levels of pH, it is

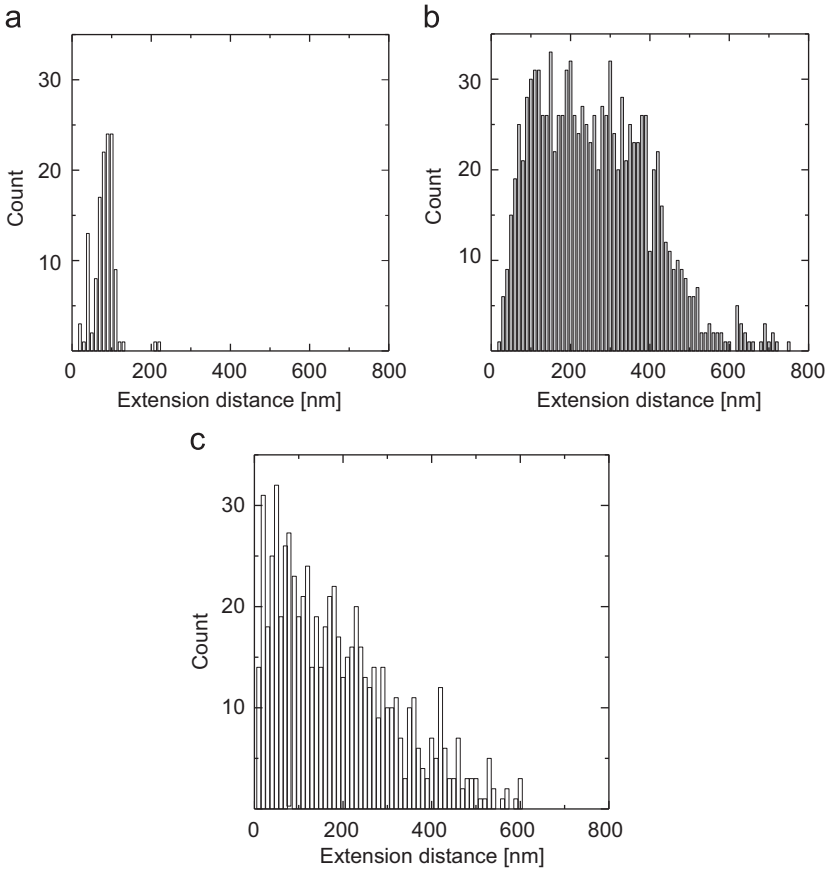

Fig. 5. Extension distance distribution of PVA. The pH of the suspension was (a) 3, (b) 6, and (c) 10.

easiest for PVA to build bridges at pH 6. Moreover, the easy bridging is thought to result from the conformation difference of PVA because the adsorbed amount of PVA was fairly constant irrespective of the pH level, as presented in Fig. 2. At pH 3, extensions were observed primarily at 90 nm and did not occur at more than 230 nm, which show good agreement with the FE-SEM micrograph showing that PVA adsorbed flatly onto the solid surface (Fig. 3(a)). At pH 6, the extensions were widely distributed from 50 nm to 450 nm and were also observed at greater than 600 nm distance. At pH 10, the peak of the extension was at approximately 50 nm, and the numbers decreased as the separation distance increased. It is also thought that the conformation of PVA at pH 6 is stretched more than that of PVA at pH 3. However, repulsion is very strong at pH 10; the number of PVA bridges between solid surfaces decreases, and it is assumed that the non-bridging PVA agglomerates and forms the sheet shape, as shown in Fig. 3(c). Consequently, the conformation of PVA changes relative to pH indicates that the bridging structure of PVA between the solid surfaces depends on the PVA conformation.

3.3. Evaluation of the PVA–PAA system

Fig. 6 shows the relation between the PAA concentration and the static contact angle of the PAA solution on the sapphire substrate. The contact angle decreased concomitantly with increasing PAA concentration from approximately 23 (0.01 mass%) to approximately 5° (0.1 mass%).

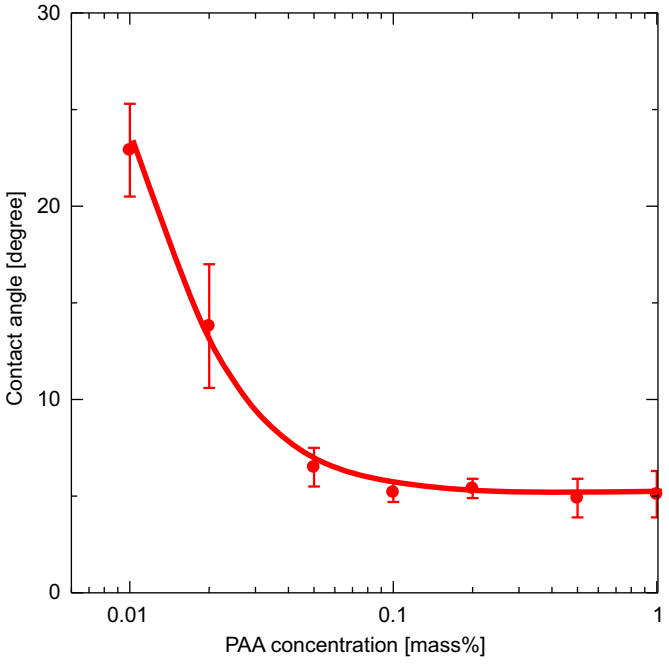

Fig. 6. Contact angle of the PAA solution on the sapphire substrate as a function of PAA concentration.

The contact angle was constant at 5° when the PAA aqueous solution was greater than 0.1 mass%. PAA adsorbing on the sapphire surface improves the sapphire surface hydrophilicity because PAA is a type of surfactant, which indicates that the decrease of the contact angle originated with the increase of the amount of PAA adsorbed at less than 0.1 mass%, and that the constant contact angle reflects satiation of the PAA adsorption at 0.1 mass% and above.

The force curve measurement results for the 0.1 mass% PAA solution are presented in Fig. 7(a). For comparison, the force curve measured in ion-exchanged purified water is also illustrated (Fig. 7(b)). The approach curve shows a slight repulsive force at approximately 20 nm caused by the electrical double layer. The long-range attractive interaction is observed, which is followed by sudden jump-in. Because of the van der Waals force, a strong adhesion force was observed when the colloidal probe was peeled from the sapphire substrate. This strong adhesion supports the contention that the interaction force in the water without polymers is explainable by the DLVO theory. In contrast, the interaction was repulsive at separation distances of less than 30 nm, and no adhesion between surfaces was observed. The repulsion is probably attributable to the PAA adsorbed onto the solid surface. Fig. 8 presents the force curve measured in the PVA–PAA aqueous solution. Repulsive forces, which originate from the steric hindrance of PAA molecules adsorbing on the solid surface, were observed in all pH solutions at less than 30 nm. As portrayed in Fig. 4(b), PVA can form bridges in the pH 6 aqueous solution. However, the force curves did not have many extensions in 0.02 mass% PAA–0.1 mass%; the PAA molecule partially covered the solid surface in this aqueous solution. Consequently, the number of the adsorption sites on the solid surface was reduced. Fig. 8(b) shows that the interaction was repulsive at all separation distances. No bridging between surfaces was observed in a 0.1 mass% PAA–0.1 mass% PVA aqueous solution. In this case, PAA molecules completely covered almost all the adsorption sites, and no PVA interaction took place in the solvent. These results indicate that it was easier for PAA than for PVA to adsorb on the Al_2O_3 surface. Only PAA worked as a dispersant. The model of the structure of the paste used to obtain sheets by tape casting was described in an earlier report [28]. According to this model, the paste consists of Al_2O_3 particles, PVA molecules, PAA molecules, and water. The Al_2O_3 particles are covered with PAA molecules, and the PVA molecules float between Al_2O_3 surfaces. That study was successful in obtaining fine tapes based on this model. However, it did not verify the selective adsorption of PAA on the Al_2O_3 surface. Our present results support their model. Moreover, in that model, PVA was used as a

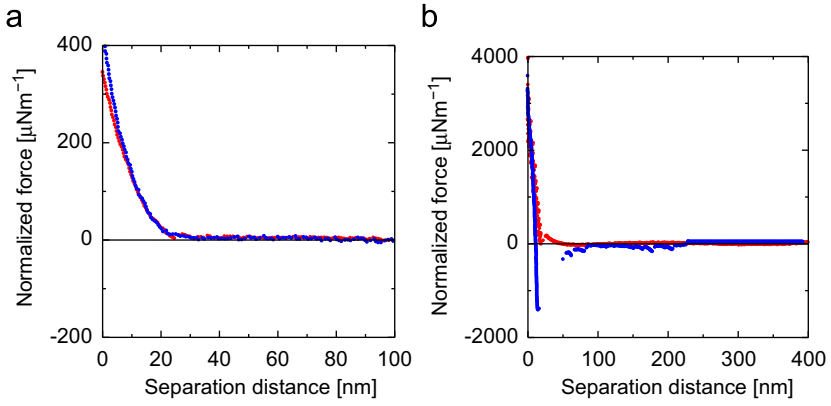

Fig. 7. Force curves measured in (a) 0.1 mass% PAA aqueous solution and (b) ion-exchanged purified water.

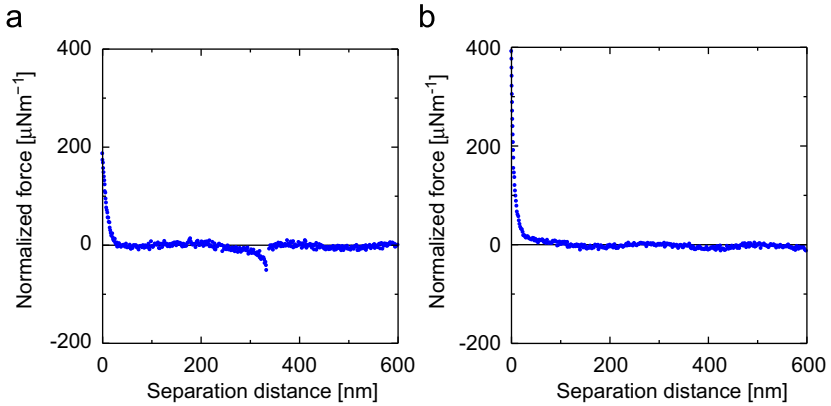

Fig. 8. Force curves measured in (a) 0.1 mass% PVA and 0.02 mass% PAA and (b) 0.1 mass% PVA and 0.2 mass% PAA aqueous solution.

binder. However, in the PVA–PAA system, PVA does not induce bridging and is thought to drift in a solvent. Therefore, it is expected that PVA mainly acts as a thickener of the solvent.

4. Summary

In this study, the adsorption and adhesion of PVA molecules on Al_2O_3 surfaces were examined in various pH or PAA aqueous solutions. First, the pH dependence of the PVA behavior was estimated. At pH 3, extensions were observed primarily at less than approximately 200 nm. In contrast, the extensions were also observed at more than approximately 600 nm at pH 6 and 10. These differences were explained by the difference of the conformation of the PVA molecule. In the PVA–PAA system, the extensions decreased by increasing the PAA content and were not observed in the 0.1 mass% PAA aqueous solution, which indicates that PAA was adsorbed more easily onto the Al_2O_3 surface than PVA and was adsorbed selectively onto the solid surface. Finally, we describe the roles played by both PVA and PAA.

PVA, which has a simple molecular structure, is a typical binder for use in wet mold processing, although its behavior is complicated. It shows different adsorption behavior in different pH solutions and might be useful as a thickener by coexistence and use with different polymers. Therefore, the organic additives for ceramics processing are understood not only by the properties of molecules but also by interaction with other additives.

Acknowledgments

We are grateful to Dr. D. Atarashi and Dr. T. Yoshioka of the Tokyo Institute of Technology for critical advice. FE-SEM micrographs were taken at the Center for Advanced Materials Analysis (CAMA) of Tokyo Institute of Technology.

References

[1] K. Holmberg, Handbook of Applied Surface and Colloid Chemistry, John Wiley and Sons, USA, 2002 1–2.
[2] J.A. Lewis, Colloidal processing of ceramics, Journal of the American Ceramic Society 83 (2000) 2341–2359.
[3] W.M. Sigmund, N.S. Bell, L. Bergström, Novel powder-processing methods for advanced ceramics, Journal of the American Ceramic Society 83 (2000) 1557–1574.
[4] Q. Li, U. Jonas, X.S. Zhao, M. Kappl, The forces at work in colloidal self-assembly: a review on fundamental interactions between colloidal particles, Asia-Pacific Journal of Chemical Engineering 3 (2008) 255–268.
[5] S. Nishimura, N. Abrams, B.A. Lewis, L.I. Halaoui, T.E. Mallouk, K.D. Benkstein, J. van de Lagemaat, A.J. Frank, Standing wave enhancement of red absorbance and photocurrent in dye-sensitized titanium dioxide photoelectrodes coupled to photonic crystals, Journal of the American Chemical Society 125 (2003) 6306–6310.
[6] L.I. Halaoui, N.M. Abrams, T.E. Mallouk, Increasing the conversion efficiency of dye-sensitized TiO_2 photoelectrochemical cells by coupling to photonic crystals, Journal of Physical Chemistry B 109 (2005) 6334–6342.
[7] S.-H.A. Lee, N.M. Abrams, P.G. Hoertz, G.D. Barber, L.I. Halaoui, T.E. Mallouk, Coupling of titania inverse opals to nanocrystalline titania layers in dye-sensitized solar cells, Journal of Physical Chemistry B 112 (2008) 14415–14421.
[8] A. Mihi, H. Míguez, Origin of light-harvesting enhancement in colloidal-photonic-crystal-based dye-sensitized solar cells, Journal of Physical Chemistry B 109 (2005) 15968–15976.
[9] A. Mihi, F.J. López-Alcaraz, H. Míguez, Full spectrum enhancement of the light harvesting efficiency of dye sensitized solar cells by including colloidal photonic crystal multilayers, Applied Physics Letters 88 (2006) 193110–193113.
[10] E.G.W. Verway, J.T.G. Overbeek, Theory of the Stability of Lyophobic Colloids, Elsevier, Amsterdam, 1948.
[11] K. Lu, C.S. Kessler, R.M. Davis, Optimization of a nanoparticle-suspension for freeze casting, Journal of the American Ceramic Society 89 (2006) 2459–2465.
[12] D.J. Shanefield, Organic Additives and Ceramic Processing: with Applications in Powder Metallurgy, Ink, and Paint, Kluwer Academic Publishers, Boston, 1996.
[13] W.A. Ducker, T.J. Senden, R.M. Pashley, Measurement of forces in liquids using a force microscope, Langmuir 8 (1992) 1831–1836.
[14] M. Polat, K. Sato, T. Nagaoka, K. Watari, Effect of pH and hydration on the normal and lateral interaction forces between alumina surfaces, Journal of Colloid and Interface Science 304 (2006) 378–387.
[15] B.C. Donose, E. Taran, I.U. Vakarelski, H. Shinto, K. Higashitani, Effects of cleaning procedures of silica wafers on their friction characteristics, Journal of Colloid and Interface Science 299 (2006) 233–237.
[16] E. Taran, B.C. Donose, I.U. Vakarelski, K. Higashitani, pH dependence of friction forces between silica surfaces in solutions, Journal of Colloid and Interface Science 297 (2006) 199–203.
[17] T. Isobe, Y. Nakagawa, M. Hayashi, S. Matsushita, A. Nakajima, Anion-specific effects on the interaction forces between Al_2O_3 surfaces and dispersibility of Al_2O_3 colloids in electrolyte solutions, Colloids and Surfaces A 396 (2012) 233–237.
[18] A. Scherer, C. Zhou, J. Michaelis, C. Brauchle, A. Zumbusch, Intermolecular interactions of polymer molecules determined by single-molecule force spectroscopy, Macromolecules 38 (2005) 9821–9825.
[19] S. Biggs, Steric and bridging forces between surfaces bearing adsorbed polymer—an atomic-force microscopy study, Langmuir 11 (1995) 156–162.
[20] H. Yilmaz, K. Sato, K. Sato, Y. Hotta, K. Watari, Lateral and normal forces in polymer-mediated interaction of alumina surfaces, Journal of the American Ceramic Society 94 (2011) 3761–3767.
[21] A. Kauppi, K.M. Andersson, L. Bergström, Probing the effect of superplaticizer adsorption on the surface forces using the colloidal probe AFM technique, Cement and Concrete Research 35 (2005) 133–140.
[22] T. Kakui, T. Miyauchi, H. Kamiya, Analysis of the action mechanism of polymer dispersant on dense ethanol alumina suspension using colloidal probe AFM, Journal of the European Ceramic Society 25 (2005) 655–661.
[23] T. Isobe, Y. Nakano, Y. Kameshima, A. Nakajima, K. Okada, AFM interaction study of poly(ammonium acrylate) adsorbed on a Si surface in KCl aqueous solution, Chemistry Letters 39 (2010) 1275–1276.
[24] T. Isobe, Y. Nakano, Y. Kameshima, A. Nakajima, K. Okada, Measurement of non-DLVO force on a silicon substrate coated with ammonium poly (acrylic acid) using scanning probe microscopy, Applied Surface Science 255 (2009) 8710–8713.
[25] A.U. Khan, P.F. Luckham, S. Manimaaran, M. Rivenet, The strength of colloidal interactions in the presence of ceramic dispersants and binders, Journal of Materials Chemistry 12 (2002) 1743–1747.

[26] A. Milling, S. Biggs, Direct measurement of the depletion force using an atomic force microscope, Journal of Colloid and Interface Science 170 (1995) 604–606.
[27] S.M. Notley, Y.-K. Leong, Interaction between silica in the presence of adsorbed poly(ethyleneimine): correlation between colloidal probe adhesion measurements and yield stress, Physical Chemistry Chemical Physics 12 (2010) 10594–10601.
[28] T. Isobe, Y. Hotta, K. Watari, Preparation of Al_2O_3 sheets from nanosized particles by aqueous tape casting, Journal of the American Ceramic Society 90 (2007) 3720–3724.